Cellular Signalling 39 (2017) 9–17

Contents lists available at ScienceDirect

Cellular Signalling

journal homepage: www.elsevier.com/locate/cellsig

HSP90 is necessary for the ACK1-dependent phosphorylation of STAT1 and STAT3

Nisintha Mahendrarajah[a], Marina E. Borisova[b], Sigrid Reichardt[c], Maren Godmann[c], Andreas Sellmer[d], Siavosh Mahboobi[d], Andrea Haitel[e], Katharina Schmid[f], Lukas Kenner[e,g,h], Thorsten Heinzel[c], Petra Beli[b], Oliver H. Krämer[a,*]

[a] Department of Toxicology, University Medical Center, Obere Zahlbacher Str. 67, 55131 Mainz, Germany
[b] Institute of Molecular Biology (IMB), Ackermannweg 4, 55128 Mainz, Germany
[c] Center for Molecular Biomedicine (CMB), Institute for Biochemistry, Friedrich-Schiller University Jena, Hans-Knöll Str. 2, 07745 Jena, Germany
[d] Institute of Pharmacy, Faculty of Chemistry and Pharmacy, University of Regensburg, 93040 Regensburg, Germany
[e] Department of Pathology, Medical University of Vienna, Waehringer Guertel 18-20, 1090 Vienna, Austria
[f] Institute of Anatomy and Experimental Morphology, University of Hamburg-Eppendorf, Martinistraße 52, 20251 Hamburg, Germany
[g] Department of Laboratory Animal Pathology, University of Veterinary Medicine, Veterinaerplatz 1, 1210 Vienna, Austria
[h] Ludwig Boltzmann Institute for Cancer Research, Waehringerstrasse 13A, 1090 Vienna, Austria

ARTICLE INFO

Keywords:
ACK1
HSP90
Lung cancer
SIAH2
STAT1
STAT3

ABSTRACT

Signal transducers and activators of transcription (STATs) are latent, cytoplasmic transcription factors. Janus kinases (JAKs) and activated CDC42-associated kinase-1 (ACK1/TNK2) catalyse the phosphorylation of STAT1 and the expression of its target genes. Here we demonstrate that catalytically active ACK1 promotes the phosphorylation and nuclear accumulation of STAT1 in transformed kidney cells. These processes are associated with STAT1-dependent gene expression and an interaction between endogenous STAT1 and ACK1. Moreover, the E3 ubiquitin ligase seven-in-absentia homolog-2 (SIAH2), which targets ACK1 through valine-909 for proteasomal degradation, attenuates the ACK1-STAT1 signalling node. We further show that ACK1 promotes the phosphorylation and nuclear accumulation of STAT3 in cultured cells and that the levels of ACK1 correlate positively with the levels of tyrosine phosphorylated STAT3 in primary lung adenocarcinoma (ADC) cells. Global analysis of ACK1 interaction partners validated the interaction of ACK1 with heat shock protein 90 (HSP90α/β). Inhibition of this chaperone with the novel drug Onalespib (AT13387) demonstrates that HSP90 is an upstream regulator of the ACK1-dependent phosphorylation of STAT1 and STAT3. In addition to these molecular insights, our data offer a pharmacological strategy to control the ACK1-STAT signalling axis.

1. Introduction

Mammalian cells express the seven STAT family members STAT1, −2, −3, −4, −5A, −5B, and −6 [1,2]. All STATs exert physiologically important roles as homo- and heterodimers [2–4]. Cytokines and growth factors activate STATs through the activation of kinases that phosphorylate serine and tyrosine residues in the C-terminal domains of STATs [2,5]. Additional posttranslational modifications critically control the activity of STATs [3,6–9].

Tyrosine phosphorylation is the best-characterized and most activating posttranslational modification of STATs. Upon binding of a cognate ligand to its receptor, receptor-associated JAKs (JAK1–3 and TYK2) catalyse the phosphorylation of STATs. This leads to an avid interaction between the phosphorylated tyrosine and the Src homology-2 (SH2) domains of two STAT molecules and the nuclear import of such dimers [1,2]. These attach to specific chromatin regions, where they recruit the transcription machinery to activate gene expression [1,2,6]. The N-terminal domains of STATs confer a weaker, but detectable interaction of STATs *in vivo* [2–4].

Recent evidence shows that ACK1 is a further kinase that can induce the tyrosine phosphorylation of STAT1 and subsequent STAT1-dependent gene expression in liver cells [10]. Like JAKs, ACK1 is a mammalian non-receptor tyrosine kinase that contributes to important physiological processes and to severe human diseases including cancer [11]. Cytokines like epidermal growth factor and platelet-derived growth factor as well as integrin β1 activation are among the stimuli that promote the phosphorylation-dependent activation of ACK1 and subsequent downstream signalling [12].

* Corresponding author.
E-mail address: okraemer@uni-mainz.de (O.H. Krämer).

http://dx.doi.org/10.1016/j.cellsig.2017.07.014
Received 25 May 2017; Received in revised form 7 July 2017; Accepted 19 July 2017
Available online 21 July 2017

Various pathways control the stability of ACK1. These include lysosomal and proteasomal degradation pathways that involve the E3 ubiquitin ligases neural-precursor-cell-expressed, developmentally-downregulated and the seven-in-absentia homologues SIAH1/SIAH2, respectively [11–14]. HSP90β also regulates the activity of ACK1 and its pro-tumourigenic functions [15].

ACK1 phosphorylates and activates STAT1 in liver-derived cells [10], but it has not been resolved which regulators of ACK1 modulate this effect. Furthermore, ACK1 might also phosphorylate other STATs. Here we demonstrate that catalytically active ACK1 induces the tyrosine phosphorylation of STAT1 and STAT3. We additionally show that active HSP90 is required for the ACK1-dependent phosphorylation of STAT1/STAT3 in cultured human cells. Furthermore, our data suggest that ACK1 phosphorylates STAT3 in primary lung cancer samples.

2. Material and methods

2.1. Cell lines

The human embryonic kidney cell line HEK293T was maintained in DMEM containing 2 mM L-glutamine, 10% foetal calf serum (FCS) and 1% penicillin/streptomycin in a humidified incubator at 37 °C and 5% CO_2. For Stable Isotope Labelling by Amino Acids in Cell Culture (SILAC), cells were cultured in media containing L-arginine (13C6 15 N4) and L-lysine (13C6 15 N2) (Cambridge Isotope Laboratories) as described previously [16]. Every 4–8 weeks all cell lines were verified to be free of mycoplasma contamination by PCR.

2.2. Drugs

Onalespib (AT13387), which blocks ATP binding and hydrolysis by HSP90, was prepared by direct amidation of 2,4-dihydroxy-5-isopropylbenzoic acid with 5-((4-methylpiperazin-1-yl)methyl)isoindoline trihydrochloride according to [17]. Using this benzotriazole methodology, the coupling reaction can be performed in a yield of 68%, without prior protection of the hydroxy substituents [18]. Doxorubicin was from Sigma-Aldrich, and for Interferon-α (IFNα) see [19].

2.3. DNA constructs

MYC-tagged ACK1 constructs: wild-type ACK1 (MYC-ACK1wt), constitutively active (MYC-ACK1ca), SIAH-binding deficient ACK1 (MYC-ACK1V909G) and autophosphorylation-deficient ACK1 (MYC-ACK1kd) and HA-tagged wild-type SIAH2 (HA-SIAH2) are described in [13].

2.4. Transfection assays

2.4.1. Turbofect transfection

HEK293T cells were transfected with different control and ACK1 and/or SIAH2 plasmids. The transfection was performed according to the manufacturer's protocol (Thermo Fisher Scientific).

2.4.2. Polyethylenimine (PEI) transfection

HEK293T cells were transfected with PEI (stock solution: 10 mM, Sigma-Aldrich) and different DNA constructs. 15 µL PBS were mixed with 2.7 µL PEI and incubated for 15–20 min at RT. Then a mixture of 15 µL PBS and 1 µg DNA was added to the PBS/PEI solution and further incubated for 30 min at RT. Then the whole mixture was added dropwise to the cells in serum-free DMEM medium without any supplements for transfection. After an incubation time of 4 h, the transfection medium was exchanged with DMEM containing FCS and antibiotics. Cells were cultivated for 48 h and used for further analyses.

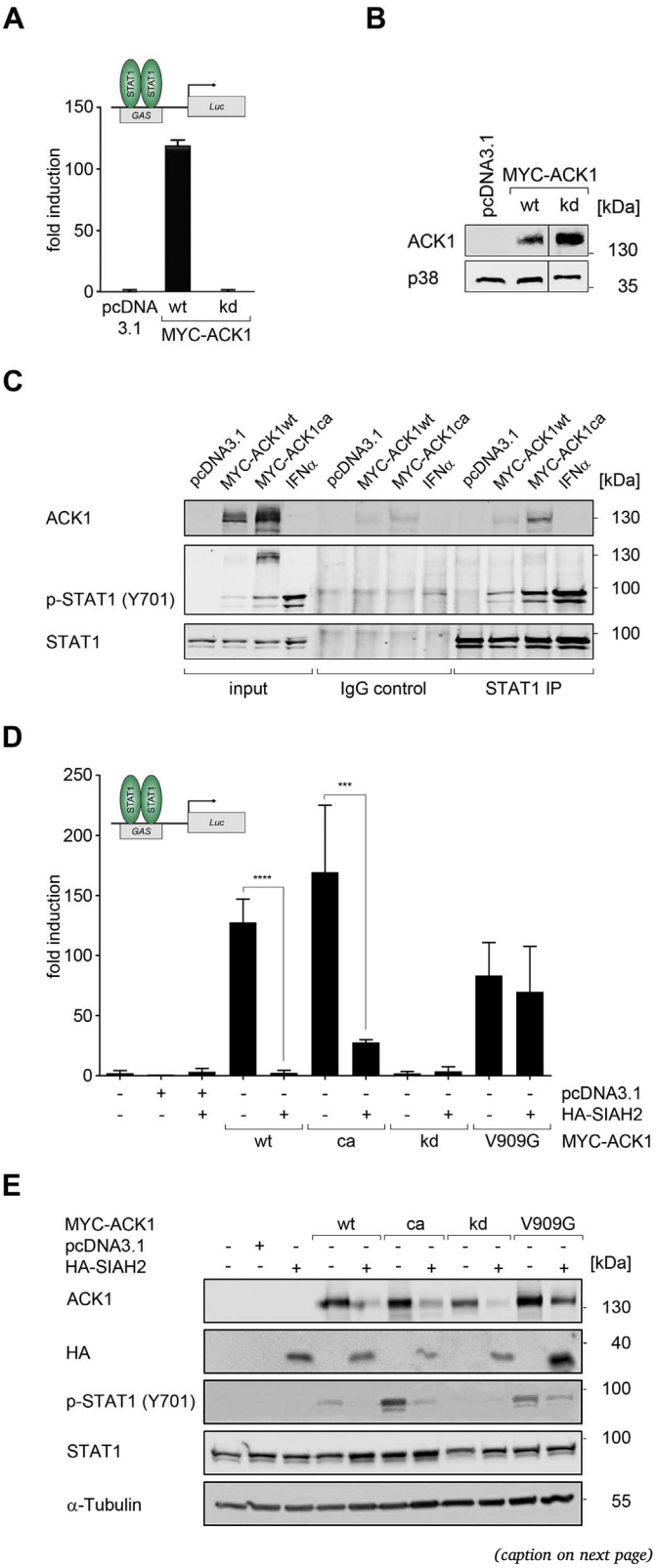

(caption on next page)

2.5. Luciferase reporter assay

This assay was performed similarly as stated in [19,20].

Fig. 1A: HEK293T cells were seeded into 24-well plates at 1 × 10^5 cells in 500 µL medium/well. 24 h later, cells in each well were transfected with 0.2 µg GAS-Luc reporter (GAS, Interferon-ɣ-activated sequence), 0.1 µg SV40-β-Gal and 0.2 µg MYC-ACK1wt, MYC-ACK1kd or

Fig. 1. ACK1-dependent activation of STAT1 is counteracted by SIAH2
(A) Catalytically active ACK1 can induce a STAT1-dependent GAS-Luc reporter in HEK293T cells. Cells were transfected with the empty control vector pcDNA3.1, MYC-tagged wildtype ACK1 (MYC-ACK1wt) or autophosphorylation-deficient ACK1 (MYC-ACK1kd); n = 3 ± SD. (B) Immunoblot detection of ACK1 in whole cell extracts of HEK293T cells transfected as noted; p38, loading control. (C) ACK1 binds STAT1. STAT1 IPs of HEK293T cells transfected as noted were analysed by immunoblotting for ACK1, pY701-STAT1 and STAT1 (IgG, irrelevant pre-immune control serum IPs). Please note that in whole cell extracts (inputs) of HEK293T cells transfected with constitutively active ACK1, ACK1 is co-detected by the p-STAT1 antibody. This does not influence the IP of STAT1, as the STAT1 antibody does not cross-react with ACK1. Cells cultivated in the presence of IFNα for 30 min serves as a positive control for phosphorylated STAT1. (D) SIAH2 blocks ACK1/STAT1-dependent activation of the GAS-Luc reporter in HEK293T cells transfected as stated; HA-tagged wildtype SIAH2 (HA-SIAH2), constitutively active ACK1 (MYC-ACK1ca), SIAH-binding deficient ACK1 (MYC-ACK1V909G); n = 3 ± SD; one-way ANOVA, Bonferroni's multiple comparisons test; ***P ≤ 0.001, ****P ≤ 0.0001. (E) Analysis of ACK1, HA-tagged SIAH2, pY701-STAT1 and STAT1 by immunoblotting in lysates of HEK293T cells transfected as stated; α-Tubulin, loading control.

with the empty vector pcDNA3.1 used to obtain equal amounts of transfected DNA with PEI.

Fig. 1D: HEK293T cells were seeded as described above. Cells were transfected with 0.1 μg GAS-Luc, 0.05 μg SV40-β-Gal and 0.1 μg pcDNA3.1 or MYC-ACK1wt/ca/kd/V909G and co-transfected with 0.1 μg HA-SIAH2 with Turbofect.

Fig. 3C: HEK293T cells were seeded into 12-well plates at 2×10^5 cells in 1 mL medium/well. Cells were transfected with 0.4 μg GAS-Luc, 0.4 μg pcDNA3.1 and 0.2 μg SV40-β-Gal with PEI. 24 h after transfection cells were treated with Doxorubicin (1 μM, 2/6 h; 2 μM, 24 h).

After a transfection period of 48 h the activity of the GAS-Luc reporter was measured and it was normalized to the constitutively expressed β-galactosidase activity. Samples of these cells were also used for immunoblot analyses. Luciferase reporter experiments were performed as triplicates.

2.6. Immunoblot

HEK293T cells were seeded into 100 mm dishes at a density of 2×10^6 cells in 10 mL medium. After 24 h, cells were transfected (Turbofect/PEI) with 10 μg pcDNA3.1/GFP, MYC-ACK1wt, MYC-ACK1ca for 48 h. Cells were harvested with trypsin and used to prepare whole cell extracts or cytoplasmic/nuclear extracts (see Section 2.7). Preparation of whole cell extracts, SDS-PAGE and immunoblotting are further described in [13,21].

Antibodies for immunoblot analyses were purchased from Abcam: α-Tubulin, ab176560; BD Pharmingen: PARP-1/556362; Cell Signaling Technology: p38/9212; pS139-H2AX/9718; Covance: HA.11 Clone 16B12/MMS-101P; Enzo Life Sciences: HSP90/ADI-SPA-830-F; Merck Millipore: pY284-ACK1/09–142; acetyl-Histone H3/06–599; Santa Cruz Biotechnology: ACK1/sc-28,336; β-Actin/sc-47,778; HSP90α/β/sc-13,119; STAT1 p84/p91/sc-346; pY701-STAT1/sc-7988; STAT3/sc-482; pY705-STAT3/sc-7993-R; pY, phosphorylated tyrosine residue.

2.7. Preparation of cytoplasmic and nuclear extracts

HEK293T cells were transfected with GFP, MYC-ACK1wt and MYC-ACK1ca plasmids (Turbofect). After 48 h cells were harvested by trypsinization and washed with PBS. The cell pellets were frozen away at − 80 °C. Following steps were performed on ice. The pellets were resuspended in 125 μL of lysis buffer A (10 mM HEPES-KOH (pH 7.9), 1.5 mM $MgCl_2$, 10 mM KCl, 1 mM DTT, 1 × protease-inhibitor-cocktail, 1 mM Na_3VO_4, 2 mM NaF). To resuspend the cells, the Eppendorf tubes were flicked with fingers. The samples were incubated for 15 min and then 12.5 μL 10% NP-40 were added to lyse all membranes, except the nuclear membrane. After 30 s vortexing the samples were centrifuged at 3.000 × g and 4 °C. The supernatant, which represents the cytoplasmic fraction, was transferred into a new 1.5 mL Eppendorf tube. The remaining pellet was resuspended gently in 500 μL isotonic buffer (10 mM Tris-HCl [pH 7.4], 150 mM NaCl). After centrifugation, the isotonic fraction was discarded.

To prepare the nuclear fraction, the pellet was resuspended thoroughly in 45 μL lysis buffer B (20 mM HEPES-KOH [pH 7.9], 420 mM NaCl, 1.5 mM $MgCl_2$, 0.5 mM EDTA, 25% glycerol, 1 × protease-inhibitor-cocktail, 1 mM Na_3VO_4, 2 mM NaF) by brushing the bottom of the tube along a steel rack. During the incubation time of 20 min, the samples were resuspended 3 times. They were centrifuged for 10 min at 20.000 × g and 4 °C. This time the supernatant represented the nuclear fraction which again was transferred into a new Eppendorf tube. The samples were snap-frozen in liquid nitrogen and kept at − 80 °C until immunoblot analysis. For SDS-PAGE, 30 μL of cytoplasmic extracts and 10 μL of nuclear extracts were used.

For the experiment with AT13387, HEK293T cells were transfected (PEI) with pcDNA3.1 or MYC-ACK1ca for 24 h, then reseeded on 60 mm dishes (0.5×10^6/3 mL) and subsequently treated with 0.5–1 μM AT13387 (10 mM stock solution) for 24 h. Cytoplasmic extracts were used for immunoblot analyses.

2.8. Immunohistochemistry (IHC) for ACK1 and phosphorylated STAT3 (p-STAT3) in ADC

The different samples were obtained from previously evaluated ADC formalin-fixed paraffin-embedded specimens *via* a Galileo TMA CK Series - HTS Tissue computer assisted TMA Microarray Platform (Integrated Systems Engineering Srl, Milan, Italy). The samples measured 2 mm in diameter and 4–6 mm in length, with previously performed H & E staining to verify the histology (similarly as reported in [22]). IHC for ACK1 and p-STAT3 (104 ADC patients) was done as described in [23]. The protocol was performed according to the manufacturer's guidelines. Appropriate positive controls and negative controls were used. Samples were analysed using an Olympus BH-2 microscope. All samples were evaluated by a pathologist (K.S.; see Fig. 2B for representative samples). The average of the core stains was used to determine staining intensity.

2.9. Immunoprecipitation (IP) of STAT1

HEK293T cells were transfected (PEI) with pcDNA3.1, MYC-ACK1wt or MYC-ACK1ca. Another sample was treated only with 3000 U/mL IFNα for 30 min. It served as a positive control for STAT1 phosphorylation at Y701. 48 h after transfection, cells were harvested and lysed in NETN lysis buffer, which was supplemented with protease and phosphatase inhibitors. For IP of STAT1, 500 μg of whole cell extracts were used per condition. Sample volumes were adjusted to 500 μL with NETN buffer and incubated overnight at 4 °C on a vertical rotator either with 0.5 μg IgG rabbit (negative control, sc-2027) or with 0.5 μg STAT1 (sc-346) antibody. For each sample (pcDNA3.1, MYC-ACK1wt, MYC-ACK1ca, IFNα) we prepared two aliquots, an IgG control, and a STAT1 IP aliquot. 24 h later, 50 μL protein sepharose G beads (4 Fast Flow, GE Healthcare) were added to each sample and samples were incubated for 4 h at 4 °C. Afterwards, beads were washed 3 times with lysis buffer and the bound proteins were eluted by adding 50 μL 2 × sample buffer (RotiLoad1, ROTH) and heating at 95 °C for 10 min. SDS-PAGE was performed with 5 μg input of the whole cell extracts and 20 μL of the IPs.

2.10. Proteomics

2.10.1. Cultivation and transfection of HEK293T cells in SILAC medium

To identify new interaction partners of ACK1, we performed a quantitative proteomic analysis using a mass spectrometric method based on SILAC. Fig. 4A shows a scheme of the SILAC workflow. For SILAC labelling, cells were cultured either in heavy SILAC medium containing dialyzed FCS, L-glutamine and the isotopically labelled L-

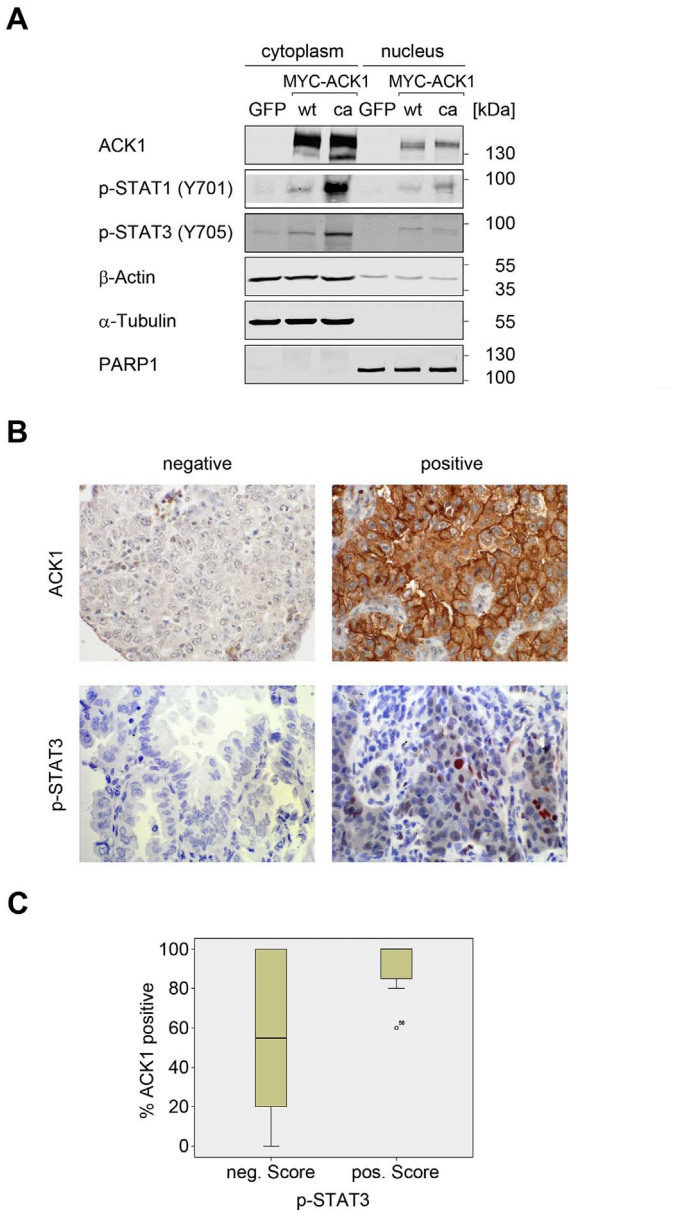

Fig. 2. ACK1 induces phosphorylation of STAT1 and STAT3
(A) ACK1 evokes the phosphorylation of STAT1 and STAT3. HEK293T cells were transfected as indicated. Cytoplasmic and nuclear extracts thereof were analysed by immunoblotting for ACK1, pY701-STAT1 and pY705-STAT3 levels. β-Actin, α-Tubulin and PARP1 served as controls for loading and fractionation. (B) IHC staining of ACK1 and p-STAT3 expression in ADC tissues. Representative pictures are shown for negative and positive expression of ACK1 and p-STAT3. (C) Samples from 104 ADC patients (Vienna patient cohort) were used for statistical evaluation. ACK1 is positively associated with p-STAT3 (box plot); Mann-Whitney-*U* test, P = 0.011; Y-axis: Percentage of ACK1 positive cells; X-axis: p-STAT3 staining intensity (negative *vs.* positive Score).

arginine (R10 = 13C6 15 N4) and L-lysine (K8 = 13C6 15 N2) or in light SILAC medium containing dialyzed FCS, L-glutamine and the natural amino acids L-arginine (R0) and L-lysine (K0).

HEK293T cells adapted to DMEM were cultivated for five doublings (~10 days) in R10K8 (heavy) and R0K0 (light) SILAC medium. After complete incorporation of light and heavy amino acids, light isotope labelled cells were transfected (PEI) with empty vector (pcDNA3.1) and heavy isotope labelled cells with the plasmid encoding MYC-ACK1ca. 48 h later, cells from each sample were harvested and lysed with modified RIPA lysis buffer (50 mM Tris-HCl (pH 7.5), 150 mM NaCl, 1 mM EDTA, 1% NP-40, 0.1% Na-deoxycholate) supplemented with protease- and phosphatase inhibitors. Protein concentrations were measured using the Bradford assay. A small amount of the lysates was saved for input (immunoblot).

2.10.2. IP of MYC-tagged ACK1

For IP, 500 µg of total protein lysate and 15 µL MYC antibody-tagged beads (7.5 µg antibody, Clontech) were used. Sample volumes were adjusted to 500 µL with modified RIPA lysis buffer and incubated with MYC antibody-tagged beads overnight at 4 °C on a vertical rotator. After 24 h, beads from light (pcDNA3.1) and heavy (MYC-ACK1ca) SILAC states were washed 4 times with lysis buffer. As the bound proteins were eluted with different lysis buffers, the beads were divided in a ratio of 1:2 for immunoblot and mass spectrometric analyses. As a negative control for the MYC IPs, we analogously prepared a further sample with 500 µg of total protein lysate and 7.5 µg IgG mouse.

For immunoblot analysis 50 µL 2 × sample buffer were added to the protein bound beads, which were subsequently heated at 95 °C for 10 min. The samples were stored at − 20 °C until analysis.

For the mass spectrometric analysis, we combined beads from two independent MYC IPs. The fifth washing step with PBS was performed on the combined beads from light and heavy SILAC states followed by the addition of NuPAGE LDS sample buffer (Life Technologies) supplemented with 1 mM DTT. Proteins were eluted by heating at 70 °C for 10 min and alkylated with 5.5 mM chloroacetamide for 30 min prior to loading on the SDS-PAGE and in-gel digestion. The label incorporation test was done with the cells prior to the IP.

2.10.3. Mass spectrometric analysis and peptide identification

Peptide fractions were analysed on a quadrupole Orbitrap mass spectrometer (Q Exactive Plus, Thermo Scientific) equipped with a UHPLC system (EASY-nLC 1000, Thermo Scientific) as described in [24]. Raw data files were analysed using MaxQuant (development version 1.5.2.8) [25]. Parent ion and MS2 spectra were searched against a database containing 88,473 human protein sequences obtained from the UniProtKB released in December 2013 using Andromeda search engine [26]. Spectra were searched with a mass tolerance of 6 ppm in MS mode, 20 ppm in HCD MS2 mode, strict trypsin specificity and allowing up to three miscleavages. Cysteine carbamidomethylation was searched as a fixed modification, whereas protein N-terminal acetylation and methionine oxidation were searched as variable modifications.

2.11. Verification of the interaction between ACK1-HSP90 by co-IP

IP of MYC-tagged ACK1 and HSP90 was performed as described before (see Section 2.9 and 2.10.2) with the following modifications: Cells were lysed with co-IP buffer (50 mM HEPES, 0.15 M NaCl, 1 mM EDTA, 0.5% NP-40, 40 mM β-Glycerophosphat, 1 mM DTT; pH 7,4) supplemented with protease- and phosphatase inhibitors. For IP of HSP90, 5 µg of anti-HSP90α/β antibody (sc-13,119) and 60 µL protein sepharose G beads were used. IP of MYC-ACK1 was carried out with 15 µL of MYC antibody-tagged beads. Precipitates formed with the antibodies were eluted with 50 µL (MYC-ACK1 IP) or 120 µL (HSP90 IP) of 6 × sample buffer (375 mM Tris-HCl (pH 6.8), 12% SDS, 30% Glycerin, 500 mM DTT, 0,01% bromphenolblue) at 95 °C for 10 min. SDS-PAGE was performed with 12.5 µg input of the whole cell extracts and 25 µL of the IPs.

2.12. Statistical analyses

For the experiments with HEK293T cells statistical analyses were carried out with one-way/two-way ANOVA and Bonferroni's/Dunnett's multiple comparisons tests. All analyses were performed with GraphPad Prism 6. For the experiments with ADC tissues statistical analyses comparing staining results IBM SPSS Statistics 22 was used. Percentage of positive tumour cells in different subgroups was compared by Mann-Whitney-*U* test (P ≤ 0.05: significant).

3. Results

3.1. Catalytically active ACK1 triggers STAT1-dependent gene expression

We set out to investigate the interplay between ACK1 and STAT1. The GAS-Luc reporter measures the induction of STAT1-dependent gene expression [19,20]. Transfection of HEK293T cells with wild-type ACK1 and the reporter led to an over 100-fold induction of the reporter (Fig. 1A). The expression of ACK1 lacking catalytic activity (ACK1kd) did not induce the reporter. Hence, ACK1 activates STAT1 through its kinase activity. We verified the overexpression of both ACK1 variants by immunoblot (Fig. 1B).

As the phosphorylation of STAT1 by its kinases requires protein-protein interactions, we tested whether STAT1 and ACK1 could be co-precipitated. We overexpressed wild-type ACK1 and constitutively active ACK1 in HEK293T cells and isolated STAT1 by IP. We immunoblotted for the presence of ACK1, tyrosine phosphorylated STAT1 (p-STAT1, phosphorylated at residue Y701) and STAT1 in such precipitates (Fig. 1C). We found that ACK1 and STAT1 could be co-precipitated. The cytokine Interferon-α (IFNα) did not promote an interaction between STAT1 and ACK1 (Fig. 1C).

These data demonstrate that ACK1 can activate and interact with STAT1.

3.2. Inhibition of the ACK1-STAT1 signalling node by SIAH2

Next, we tested if the proteasomal elimination of ACK1 *via* the E3 ubiquitin ligase SIAH2 [13] could affect the ACK1-dependent activation of the GAS-Luc reporter. Overexpression of SIAH2 blocked the ACK1-induced stimulation of the GAS-Luc reporter by wild-type and constitutively active ACK1 significantly (Fig. 1D). Overexpression of an ACK1 mutant lacking the binding site for its E3 ubiquitin ligases SIAH1/SIAH2 (ACK1V909G) [13] also induced the reporter, but SIAH2 did not suppress this process (Fig. 1D).

Whole cell extracts of these cells were immunoblotted against ACK1, p-STAT1 and STAT1. Phosphorylated STAT1 was detectable in lysates with overexpressed wild-type ACK1, ACK1V909G and constitutively active ACK1. Co-transfection of SIAH2 led to a reduction of ACK1, which was less pronounced for ACK1V909G (Fig. 1E and see [13]). While the SIAH2-dependent decrease of ACK1 was associated with a loss of p-STAT1, p-STAT1 was still detectable when ACK1V909G and SIAH2 were expressed together (Fig. 1E). SIAH2 did not affect the levels of STAT1 (Fig. 1E).

The lower activation of the GAS-Luc reporter by ACK1V909G compared to wild-type ACK1 (Fig. 1D) was not due to lower expression levels of ACK1V909G (Fig. 1E), but rather an intrinsic lower activity of this ACK1 isoform.

These findings illustrate that ACK1 promotes STAT1-dependent gene expression, which can be blocked by the E3 ubiquitin ligase SIAH2.

3.3. ACK1 induces p-STAT1 and p-STAT3 and their accumulation in the nucleus

ACK1 phosphorylated endogenous STAT1 to levels that are detectable by immunoblotting of cell extracts (Fig. 1C). We used a biochemical fractionation method to test for an accumulation of p-STAT1 in the nucleus. We transfected HEK293T cells with wild-type ACK1 or constitutively active ACK1 and separated the cells into cytoplasmic and nuclear fractions. These were then analysed by immunoblotting. We found that wild-type ACK1 and to a larger extent constitutively active ACK1 increased the phosphorylation of cytoplasmic STAT1 at Y701. This was associated with an accumulation of nuclear p-STAT1 (Fig. 2A). A minor portion of ACK1 located to the nucleus (Fig. 2A).

Since STAT1 and STAT3 are structurally related [3], we also assessed if ACK1 could induce the phosphorylation of STAT3 at residue Y705 (p-STAT3). Indeed, constitutively active ACK1 and to a lesser extent wild-type ACK1 promoted the accumulation of p-STAT3 in cytoplasm and nucleus (Fig. 2A).

To check whether ACK1 levels correlate with increased phosphorylation of STAT3 at Y705 *in vivo*, we analysed primary ADC of the lung. We only examined ADC, because these tumours carry elevated levels of p-STAT3 and low levels of SIAH2 [27]. This analysis revealed that ADC samples were positive or negative for ACK1 and p-STAT3, respectively (Fig. 2B). A subset of samples showed high levels of ACK1 which correlated with the phosphorylation of STAT3 (Fig. 2C).

These data reveal that ACK1 induces the phosphorylation of STAT1 and STAT3.

3.4. ACK1 does not evoke DNA damage signalling

ACK1 can exert oncogenic properties and induces STAT1 [10,11]. Oncogenes can induce replicative stress and DNA damage [27], which may be associated with an activation of STAT1 [28]. Therefore, we investigated whether ACK1 could induce DNA damage. We transfected HEK293T cells with either wild-type or constitutively active ACK1. Lysates of these cells were immunoblotted for the phosphorylated form of histone H2AX (p-H2AX, phosphorylated at residue S139), which is a sensitive marker for replicative stress and DNA damage [27]. This experiment showed no evidence for a significant induction of p-H2AX after the transfection of ACK1 (Fig. 3A-B).

To analyse whether DNA damage could stimulate the GAS-Luc

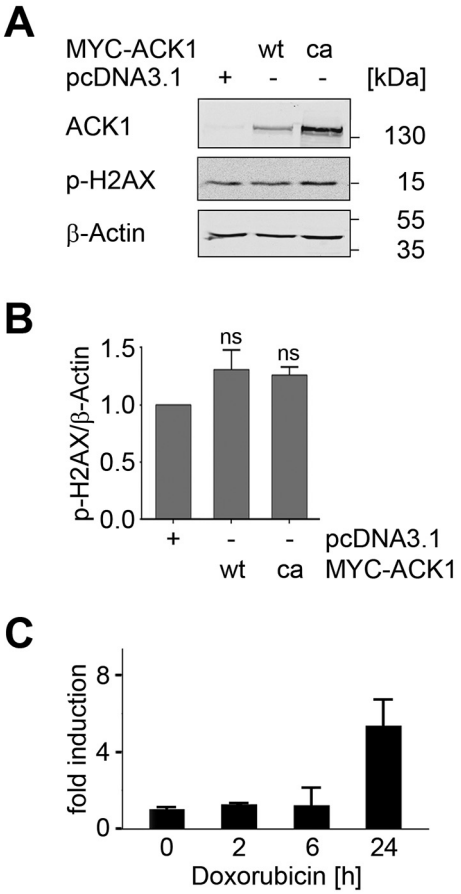

Fig. 3. No evidence for increased DNA damage upon overexpression of ACK1
(A) Active ACK1 does not cause accumulation of pS139-H2AX in HEK293T cells; β-Actin, loading control. (B) Densitometric evaluation of p-H2AX band intensity normalized to β-Actin; n = 2 ± SD; one-way ANOVA, Bonferroni's multiple comparisons test; ns, not significant. (C) Activation of the GAS-Luc reporter by Doxorubicin (1 μM for 2/6 h; 2 μM for 24 h) in HEK293T cells; n = 3 ± SD.

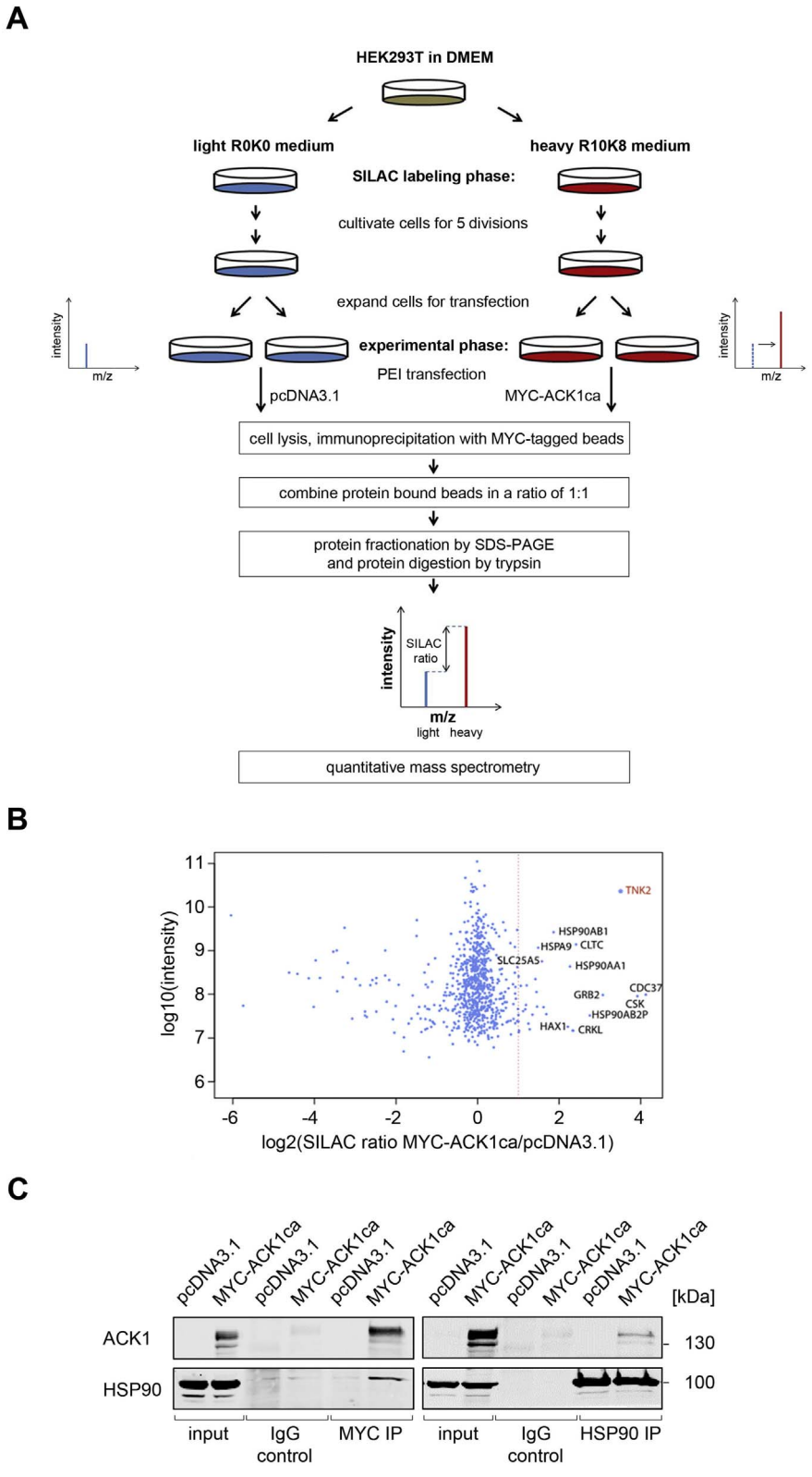

Fig. 4. A proteomic approach to identify new interaction partners of ACK1

(A) Workflow of the mass spectrometric analysis of HEK293T cells transfected with pcDNA3.1 or MYC-ACK1ca. ACK1 interaction partners were identified based on a quantitative proteomic analysis, termed Stable Isotope Labelling by Amino acids in Cell culture (SILAC). (B) Scatter plot shows logarithmized SILAC ratios of all proteins quantified in the IP. Proteins indicated right from the dotted line are enriched > 2-fold in the ACK1/TNK2 IP compared to the empty vector IP (n = 2). HSP90AA1 corresponds to HSP90α and HSP90AB1 corresponds to HSP90β. (C) Interaction of HSP90 with ACK1. MYC-tagged ACK1 and HSP90 IPs from HEK293T cells were analysed by immunoblotting for ACK1 and HSP90α/β (n = 2).

reporter, we transfected HEK293T cells with this reporter and treated the cells with the DNA-damaging drug Doxorubicin. We were able to verify that conditions evoking DNA damage activated the GAS-Luc reporter. However, the extent of activation (Fig. 3C) was distinctly less than with the transfection of ACK1 (Fig. 1A and D).

These data suggest that ACK1 does not cause DNA damage.

3.5. Global analysis of ACK1 interaction partners

Having assessed that ACK1 activates the phosphorylation of STAT1, we examined which interaction partners of ACK1 might affect this signalling node. We transfected HEK293T cells with MYC-ACK1ca and immunoprecipitated this factor using antibodies against the MYC tag (Fig. 4A). Stable isotope labelling by amino acids (SILAC) was

employed to distinguish specific interaction partners from background binders in the empty vector-transfected cells. Immunoprecipitated proteins were resolved by SDS-PAGE and digested in-gel with trypsin. Peptide samples were then analysed by liquid chromatography-tandem mass spectrometry (LC-MS/MS) (Fig. 4A).

Among the proteins that were strongly enriched in MYC-ACK1ca IPs were known and putative novel interaction partners of ACK1 (Fig. 4B and Supplementary Table S1). Heat shock proteins HSP90α and HSP90β were highly enriched in MYC-ACKca IPs in comparison to IPs performed with empty vector-transfected cells.

To verify the interaction between HSP90 and ACK1, we overexpressed MYC-ACK1ca in HEK293T cells and formed IPs with the HSP90α/β antibody or the MYC antibody-tagged beads. By Western blot, we tested for the co-precipitation of ACK1 or HSP90, respectively. This experiment verified an interaction between these proteins in both IP directions (Fig. 4C).

These results illustrate that ACK1 and HSP90 interact reciprocally in HEK293T cells.

3.6. Relevance of HSP90 for ACK1-STAT1 signalling

Since HSP90 functionally interacts with ACK1 [15], we investigated whether HSP90 affects the phosphorylation of STATs by ACK1. We transfected HEK293T cells with MYC-ACK1ca and treated the cells with the novel HSP90 inhibitor (HSP90i) AT13387 [17,18]. This agent blocks the N-terminal ATPase site of HSP90 [17,18].

We chose a concentration of AT13387 that only slightly increased apoptosis and necrosis in HEK293T cell cultures (Supplementary Fig. S1). These doses of AT13387 reduced total ACK1, p-ACK1 and the ACK1-induced phosphorylation of STAT1 (Fig. 5A-B). Moreover, A-T13387 also attenuated the phosphorylation of STAT3 by ACK1 (Fig. 5C-D).

In sum, our data illustrate that active HSP90 is necessary for the phosphorylation of STAT1 and STAT3 by the SIAH target ACK1 (Fig. 5E).

4. Discussion

Our work demonstrates that catalytically active ACK1 can promote the activation of STAT1 and STAT3. A degradation of ACK1 by SIAH2 as well as the pharmacological inhibition of HSP90 with AT13387 suppress the phosphorylation of STAT1 and STAT3. We summarize these new findings in Fig. 5E. We collected the data in a permanent human cell line and primary ADC samples. As methods, we used reporter gene assays, immunoblot, biochemical fractionation assays, IHC, and IP techniques.

It was previously reported that ACK1 could interact with overexpressed STAT1 in the human hepatoma cell line Huh7. The authors detected an ACK1-dependent phosphorylation of STAT1 when they enriched STAT1 by IP [10]. We show that an ACK1-dependent tyrosine phosphorylation of endogenous STAT1 can be detected in whole cell extracts of HEK293T cells. In addition, we demonstrate that ACK1 promotes the phosphorylation of endogenous STAT3 and the nuclear accumulation of p-STAT1 and p-STAT3. Congruent with these data, an inactivation of ACK1 with the tyrosine kinase inhibitor Dasatinib attenuates p-STAT3 [29]. Further studies will address whether ACK1 also phosphorylates STAT5, which is frequently dysregulated in ADC [30].

Moreover, we note that an ACK1 mutant that lacks a SIAH degron motif (ACK1 carrying a V909G point mutation) is less sensitive to the SIAH2-mediated inhibition of STAT1 signalling. Curiously, compared to wild-type ACK1 such a molecule is a less active inducer of STAT1-dependent gene expression in the absence of ectopically expressed SIAH2. We speculate that a low basal proteasomal turnover of ACK1 promotes its ability to phosphorylate STAT1 and that a high level of SIAH2 pushes this equilibrium towards the proteasomal destruction of ACK1. However, we cannot rule out that an association of SIAH2 with ACK1 may target additional factors that build up the molecular machinery for STAT1-dependent gene expression.

The above data are consistent with the finding that SIAH2 targets ACK1 for proteasomal degradation [13]. We reported that SIAH2 was overexpressed in primary squamous cell carcinoma of the lung [31] and others verified this finding in an independent cohort [32]. This overexpression of SIAH2 is associated with a reduced expression of TYK2, attenuated phosphorylation of STAT3, and a lower expression of its target matrix metalloproteinase-1 [31]. Therefore, SIAH2 may target ACK1 and consequently the phosphorylation and activation of STAT1 and STAT3 in lung cancer. The relevance of this finding could be identified *in vivo* and may be more complex than anticipated. While STAT3 can be a poor prognostic factor in lung cancer patients [33], STAT3 can equally act as tumour suppressor in lung and prostate cancer cells [34,35]. Furthermore, SIAH2 and ACK1 may control prostate cancer cell growth [12,14] through their antagonistic regulation of STAT-dependent gene expression.

Earlier studies revealed an interaction between HSP90β and ACK1 [15]. In the proteomic approach, we show that ACK1 associates with HSP90α and HSP90β. Additionally, we confirm the existence of a HSP90-ACK1 complex with co-IP experiments. We further analysed whether an inhibition of HSP90 affected the expression of ACK1 and the activation of STATs. We reveal that the HSP90i AT13387 diminishes ACK1 phosphorylation and its expression after 24 h. Apparently, inhibiting HSP90 leads to a disruption of the ACK1-STAT1 and ACK1-STAT3 signalling nodes due to a dephosphorylation and destabilization of ACK1. Consistent with these data, the HSP90i Geldanamycin abolished the phosphorylation of constitutively active ACK1 in the prostatic adenocarcinoma cell line LNCaP after 8 h [15]. In this experiment, the levels of ACK1 were not significantly lowered [15], which is likely due to the shorter incubation time with the HSP90i.

Notably, Geldanamycin treatment can strongly attenuate ACK1-driven LNCaP cell tumourigenesis *in vivo* [15] and epigenetic drugs of the histone deacetylase inhibitor family induce a caspase-dependent cleavage of ACK1 and a loss of p-STAT3 in leukemic cells [22]. Moreover, as ACK1 is able to promote tumour growth by regulating tumour suppressors (WWOX) and pro-survival factors (AKT) [15,36,37], ACK1 interacting partners and the regulation of STAT signalling by ACK1 appear as promising targets for cancer drug development. Such strategies might be appreciated in light of the fact that recent data illustrate an overexpression of ACK1 and its association with a worse patient outcome, *e.g.*, in pancreatic cancer [30], hepatocellular carcinoma [38], stomach cancer [39], colon cancer [40] and breast cancer [41].

AT13387, which is currently the most potent inhibitor of the N-terminal ATP site of HSP90, is active against lung cancer cells *in vitro* and *in vivo* [42]. The reduction of the ACK1-STAT3 signalling axis by this agent may serve as a novel pharmacodynamic marker for HSP90 inhibition. In addition, others found that inhibition of HSP90 attenuates the phosphorylation of STAT3 in autosomal dominant polycystic kidney disease [43]. This finding supports our results, which may have broader implications.

5. Conclusions

This work reveals that active ACK1 induces STAT1-dependent gene expression. ACK1 phosphorylates both STAT1 and STAT3. Furthermore, a reduction of ACK1 through an interaction with SIAH2 attenuates p-STAT1. Inhibition of HSP90 with AT13387 diminishes the activity of ACK and thereby the levels of p-STAT1 and p-STAT3. Thus, targeting HSP90 is a feasible approach to regulate ACK1-STAT1/STAT3 signalling.

Supplementary data to this article can be found online at http://dx.doi.org/10.1016/j.cellsig.2017.07.014.

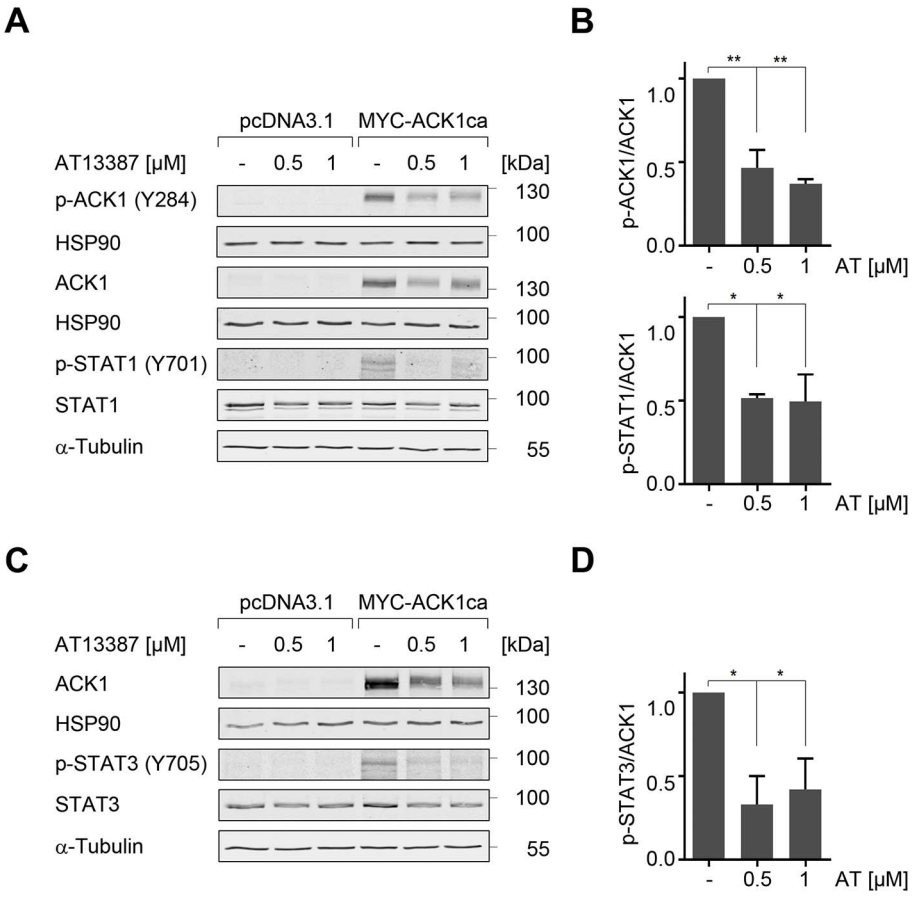

Fig. 5. HSP90 promotes the phosphorylation of STAT1 and STAT3 by ACK1

(A) Cytoplasmic extracts of HEK293T cells transfected with pcDNA3.1 or MYC-ACK1ca were treated with 0.5–1 μM AT13387 and analysed by immunoblotting for pY284-ACK1, ACK1, pY701-STAT1 and STAT1; HSP90 and α-Tubulin, loading controls. (B) Densitometric evaluation of p-ACK1 and p-STAT1 normalized to total ACK1. Untreated samples with MYC-ACK1ca were set as 1; AT, AT13387; n = 2 ± SD; one-way ANOVA, Dunnett's multiple comparisons test; *P ≤ 0.05, **P ≤ 0.01. (C) Detection of ACK1, pY705-STAT3 and STAT3. (D) Quantification of p-STAT3 normalized to ACK1; n = 2 ± SD; one-way ANOVA, Dunnett's multiple comparisons test; *P ≤ 0.05. (E) Graphical abstract: Active HSP90 is necessary for activation of STAT1 and STAT3 by ACK1. See text for further details.

Conflict of interest disclosure

The authors declare no competing financial interests.

Acknowledgements

The Wilhelm Sander-Stiftung (#2010.078 to O.H.K) supported the major part of this work. The laboratory of O.H.K is additionally supported by the Deutsche Forschungsgemeinschaft (#KR2291/4-1, KR2291/5-1 and KR2291/7-1 to O.H.K), the Deutsche Krebshilfe (#110909 and 110125 to O.H.K; German Cancer Aid) and intramural funding (University Medical Center Mainz and Naturwissenschaftlich-medizinisches Forschungszentrum Mainz, NMFZ). This work was further supported by the Austrian Science Fund (FWF-P 26011 and FWF-P 29251-B28 to L.K.) and the European Training Network (MSCA-ITN-2015-ETN ALKATRAS No 675712 to L.K.). We thank Elisabeth Gurnhofer for excellent technical assistance.

Author contributions

O.H.K. designed the project. N.M., S.R., A.H and K.S. performed the experiments. M.E.B. and P.B. performed mass spectrometry analysis. N.M., M.G., L.K., and O.H.K analysed the data. T.H., S.M., A.S., L.K., and O.H.K. provided material. N.M. and O.H.K. prepared the figures. N.M., L.K. and OHK wrote and reviewed the manuscript.

References

[1] C.I. Santos, A.P. Costa-Pereira, Signal transducers and activators of transcription-from cytokine signalling to cancer biology, Biochim. Biophys. Acta 1816 (1) (2011) 38–49.
[2] P.B. Sehgal, Paradigm shifts in the cell biology of STAT signaling, Semin. Cell Dev. Biol. 19 (4) (2008) 329–340.
[3] M. Wieczorek, T. Ginter, P. Brand, T. Heinzel, O.H. Krämer, Acetylation modulates the STAT signaling code, Cytokine Growth Factor Rev. 23 (6) (2012) 293–305.
[4] C. Mertens, M. Zhong, R. Krishnaraj, W. Zou, X. Chen, J.E. Darnell Jr., Dephosphorylation of phosphotyrosine on STAT1 dimers requires extensive spatial reorientation of the monomers facilitated by the N-terminal domain, Genes Dev. 20 (24) (2006) 3372–3381.

[5] H. Cheon, E.C. Borden, G.R. Stark, Interferons and their stimulated genes in the tumor microenvironment, Semin. Oncol. 41 (2) (2014) 156–173.
[6] K.K. Biggar, S.S. Li, Non-histone protein methylation as a regulator of cellular signalling and function, Nat. Rev. Mol. Cell Biol. 16 (1) (2015) 5–17.
[7] L. Icardi, K. De Bosscher, J. Tavernier, The HAT/HDAC interplay: multilevel control of STAT signaling, Cytokine Growth Factor Rev. 23 (6) (2012) 283–291.
[8] C. Ott, K. Jacobs, E. Haucke, A. Navarrete Santos, T. Grune, A. Simm, Role of advanced glycation end products in cellular signaling, Redox Biol. 2 (2014) 411–429.
[9] P. Freund, M.A. Kerenyi, M. Hager, T. Wagner, B. Wingelhofer, H.T. Pham, M. Elabd, X. Han, P. Valent, F. Gouilleux, V. Sexl, O.H. Krämer, B. Groner, R. Moriggl, O-GlcNAcylation of STAT5 controls tyrosine phosphorylation and oncogenic transcription in STAT5-dependent malignancies, Leukemia (2017).
[10] Y. Fujimoto, H. Ochi, T. Maekawa, H. Abe, C.N. Hayes, H. Kumada, Y. Nakamura, K. Chayama, A single nucleotide polymorphism in activated Cdc42 associated tyrosine kinase 1 influences the interferon therapy in hepatitis C patients, J. Hepatol. 54 (4) (2011) 629–639.
[11] K. Mahajan, N.P. Mahajan, ACK1/TNK2 tyrosine kinase: molecular signaling and evolving role in cancers, Oncogene 34 (32) (2015) 4162–4167.
[12] V. Prieto-Echagüe, W.T. Miller, Regulation of ack-family nonreceptor tyrosine kinases, J. Signal Transduct. 2011 (2011) 742372.
[13] M. Buchwald, K. Pietschmann, P. Brand, A. Gunther, N.P. Mahajan, T. Heinzel, O.H. Krämer, SIAH ubiquitin ligases target the nonreceptor tyrosine kinase ACK1 for ubiquitinylation and proteasomal degradation, Oncogene 32 (41) (2013) 4913–4920.
[14] S.K. Knauer, N. Mahendrarajah, W.P. Roos, O.H. Krämer, The inducible E3 ubiquitin ligases SIAH1 and SIAH2 perform critical roles in breast and prostate cancers, Cytokine Growth Factor Rev. 26 (4) (2015) 405–413.
[15] N.P. Mahajan, Y.E. Whang, J.L. Mohler, H.S. Earp, Activated tyrosine kinase Ack1 promotes prostate tumorigenesis: role of Ack1 in polyubiquitination of tumor suppressor Wwox, Cancer Res. 65 (22) (2005) 10514–10523.
[16] S.E. Ong, B. Blagoev, I. Kratchmarova, D.B. Kristensen, H. Steen, A. Pandey, M. Mann, Stable isotope labeling by amino acids in cell culture, SILAC, as a simple and accurate approach to expression proteomics, Mol. Cell. Proteomics 1 (5) (2002) 376–386.
[17] B.H. Patel, A.G. Barrett, Total synthesis of resorcinol amide Hsp90 inhibitor AT13387, J. Org. Chem. 77 (24) (2012) 11296–11301.
[18] A.J. Woodhead, H. Angove, M.G. Carr, G. Chessari, M. Congreve, J.E. Coyle, J. Cosme, B. Graham, P.J. Day, R. Downham, L. Fazal, R. Feltell, E. Figueroa, M. Frederickson, J. Lewis, R. McMenamin, C.W. Murray, M.A. O'Brien, L. Parra, S. Patel, T. Phillips, D.C. Rees, S. Rich, D.M. Smith, G. Trewartha, M. Vinkovic, B. Williams, A.J. Woolford, Discovery of (2,4-dihydroxy-5-isopropylphenyl)-[5-(4-methylpiperazin-1-ylmethyl)-1,3-dihydrois oindol-2-yl]methanone (AT13387), a novel inhibitor of the molecular chaperone Hsp90 by fragment based drug design, J. Med. Chem. 53 (16) (2010) 5956–5969.
[19] O.H. Krämer, S.K. Knauer, G. Greiner, E. Jandt, S. Reichardt, K.H. Gührs, R.H. Stauber, F.D. Böhmer, T. Heinzel, A phosphorylation-acetylation switch regulates STAT1 signaling, Genes Dev. 23 (2) (2009) 223–235.
[20] T. Ginter, C. Bier, S.K. Knauer, K. Sughra, D. Hildebrand, T. Munz, T. Liebe, R. Heller, A. Henke, R.H. Stauber, W. Reichardt, J.A. Schmid, K.F. Kubatzky, T. Heinzel, O.H. Krämer, Histone deacetylase inhibitors block IFNgamma-induced STAT1 phosphorylation, Cell. Signal. 24 (7) (2012) 1453–1460.
[21] M. Beyer, N. Kiweler, S. Mahboobi, O.H. Krämer, How to distinguish between the activity of HDAC1-3 and HDAC6 with western blot, Methods Mol. Biol. 1510 (2017) 355–364.
[22] L. Kadletz, G. Heiduschka, R. Wiebringhaus, E. Gurnhofer, U. Kotowski, G. Haymerle, M. Brunner, C. Barry, L. Kenner, ELMO3 expression indicates a poor prognosis in head and neck squamous cell carcinoma - a short report, Cell. Oncol. (2016).
[23] M. Schlederer, K.M. Mueller, J. Haybaeck, S. Heider, N. Huttary, M. Rosner, M. Hengstschlager, R. Moriggl, H. Dolznig, L. Kenner, Reliable quantification of protein expression and cellular localization in histological sections, PLoS One 9 (7) (2014) e100822.
[24] A. Michalski, E. Damoc, J.P. Hauschild, O. Lange, A. Wieghaus, A. Makarov, N. Nagaraj, J. Cox, M. Mann, S. Horning, Mass spectrometry-based proteomics using Q Exactive, a high-performance benchtop quadrupole Orbitrap mass spectrometer, Mol. Cell. Proteomics 10 (9) (2011) M111–011015.
[25] J. Cox, M. Mann, MaxQuant enables high peptide identification rates, individualized p.p.b.-range mass accuracies and proteome-wide protein quantification, Nat. Biotechnol. 26 (12) (2008) 1367–1372.
[26] J. Cox, N. Neuhauser, A. Michalski, R.A. Scheltema, J.V. Olsen, M. Mann, Andromeda: a peptide search engine integrated into the MaxQuant environment, J. Proteome Res. 10 (4) (2011) 1794–1805.
[27] M. Dobbelstein, C.S. Sørensen, Exploiting replicative stress to treat cancer, Nat. Rev. Drug Discov. 14 (6) (2015) 405–423.
[28] N.C. Schmitt, E.W. Rubel, N.M. Nathanson, Cisplatin-induced hair cell death requires STAT1 and is attenuated by epigallocatechin gallate, J. Neurosci. 29 (12) (2009) 3843–3851.
[29] N. Mahendrarajah, R. Paulus, O.H. Krämer, Histone deacetylase inhibitors induce proteolysis of activated CDC42-associated kinase-1 in leukemic cells, J. Cancer Res. Clin. Oncol. 142 (11) (2016) 2263–2273.
[30] S.G. Sanchez-Ceja, E. Reyes-Maldonado, M.E. Vazquez-Manriquez, J.J. Lopez-Luna, A. Belmont, S. Gutierrez-Castellanos, Differential expression of STAT5 and Bcl-xL, and high expression of Neu and STAT3 in non-small-cell lung carcinoma, Lung Cancer 54 (2) (2006) 163–168.
[31] S. Müller, Y. Chen, T. Ginter, C. Schäfer, M. Buchwald, L.M. Schmitz, J. Klitzsch, A. Schütz, A. Haitel, K. Schmid, R. Moriggl, L. Kenner, K. Friedrich, C. Haan, I. Petersen, T. Heinzel, O.H. Krämer, SIAH2 antagonizes TYK2-STAT3 signaling in lung carcinoma cells, Oncotarget 5 (10) (2014) 3184–3196.
[32] P. Moreno, M. Lara-Chica, R. Soler-Torronteras, T. Caro, M. Medina, A. Alvarez, A. Salvatierra, E. Munoz, M.A. Calzado, The expression of the ubiquitin ligase SIAH2 (seven in absentia homolog 2) is increased in human lung cancer, PLoS One 10 (11) (2015) e0143376.
[33] D. Harada, N. Takigawa, K. Kiura, The role of STAT3 in non-small cell lung cancer, Cancer 6 (2) (2014) 708–722.
[34] B. Grabner, D. Schramek, K.M. Mueller, H.P. Moll, J. Svinka, T. Hoffmann, E. Bauer, L. Blaas, N. Hruschka, K. Zboray, P. Stiedl, H. Nivarthi, E. Bogner, W. Gruber, T. Mohr, R.H. Zwick, L. Kenner, V. Poli, F. Aberger, D. Stoiber, G. Egger, H. Esterbauer, J. Zuber, R. Moriggl, R. Eferl, B. Gyorffy, J.M. Penninger, H. Popper, E. Casanova, Disruption of STAT3 signalling promotes KRAS-induced lung tumorigenesis, Nat. Commun. 6 (2015) 6285.
[35] J. Pencik, M. Schlederer, W. Gruber, C. Unger, S.M. Walker, A. Chalaris, I.J. Marie, M.R. Hassler, T. Javaheri, O. Aksoy, J.K. Blayney, N. Prutsch, A. Skucha, M. Herac, O.H. Krämer, P. Mazal, F. Grebien, G. Egger, V. Poli, W. Mikulits, R. Eferl, H. Esterbauer, R. Kennedy, F. Fend, M. Scharpf, M. Braun, S. Perner, D.E. Levy, T. Malcolm, S.D. Turner, A. Haitel, M. Susani, A. Moazzami, S. Rose-John, F. Aberger, O. Merkel, R. Moriggl, Z. Culig, H. Dolznig, L. Kenner, STAT3 regulated ARF expression suppresses prostate cancer metastasis, Nat. Commun. 6 (2015) 7736.
[36] K. Mahajan, D. Coppola, S. Challa, B. Fang, Y.A. Chen, W. Zhu, A.S. Lopez, J. Koomen, R.W. Engelman, C. Rivera, R.S. Muraoka-Cook, J.Q. Cheng, E. Schonbrunn, S.M. Sebti, H.S. Earp, N.P. Mahajan, Ack1 mediated AKT/PKB tyrosine 176 phosphorylation regulates its activation, PLoS One 5 (3) (2010) e9646.
[37] K. Mahajan, D. Coppola, Y.A. Chen, W. Zhu, H.R. Lawrence, N.J. Lawrence, N.P. Mahajan, Ack1 tyrosine kinase activation correlates with pancreatic cancer progression, Am. J. Pathol. 180 (4) (2012) 1386–1393.
[38] B. Wang, T. Xu, J. Liu, S. Zang, L. Gao, A. Huang, Overexpression of activated Cdc42-associated kinase1 (Ack1) predicts tumor recurrence and poor survival in human hepatocellular carcinoma, Pathol. Res. Pract. 210 (12) (2014) 787–792.
[39] S.H. Xu, J.Z. Huang, M. Chen, M. Zeng, F.Y. Zou, D. Chen, G.R. Yan, Amplification of ACK1 promotes gastric tumorigenesis via ECD dependent p53 ubiquitination degradation, Oncotarget (2015).
[40] C. Lv, X. Zhao, H. Gu, L. Huang, S. Zhou, F. Zhi, Involvement of activated Cdc42 Kinase1 in colitis and colorectal neoplasms, Med. Sci. Monit. 22 (2016) 4794–4802.
[41] X. Wu, M.S. Zahari, S. Renuse, D.S. Kelkar, M.A. Bharbuiya, P.L. Rojas, V. Stearns, E. Gabrielson, P. Malla, S. Sukumar, N.P. Mahajan, A. Pandey, The non-receptor tyrosine kinase TNK2/ACK1 is a novel therapeutic target in triple negative breast cancer, Oncotarget 8 (2) (2017) 2971–2983.
[42] B. Graham, J. Curry, T. Smyth, L. Fazal, R. Feltell, I. Harada, J. Coyle, B. Williams, M. Reule, H. Angove, D.M. Cross, J. Lyons, N.G. Wallis, N.T. Thompson, The heat shock protein 90 inhibitor, AT13387, displays a long duration of action in vitro and in vivo in non-small cell lung cancer, Cancer Sci. 103 (3) (2012) 522–527.
[43] T. Seeger-Nukpezah, D.A. Proia, B.L. Egleston, A.S. Nikonova, T. Kent, K.Q. Cai, H.-H. Hensley, W. Ying, D. Chimmanamada, I.G. Serebriiskii, E.A. Golemis, Inhibiting the HSP90 chaperone slows cyst growth in a mouse model of autosomal dominant polycystic kidney disease, Proc. Natl. Acad. Sci. U. S. A. 110 (31) (2013) 12786–12791.